Dynamics of the Fluid in a Spinning Coning Cylinder

Philip Hall*
Exeter University, Exeter, United Kingdom
and
Raymond Sedney† and Nathan Gerber††
U.S. Army Ballistic Research Laboratory, Aberdeen Proving Ground, Maryland

The fluid motion inside a cylinder that simultaneously spins and cones is determined according to linear theory for small coning angles. The Navier-Stokes equations are solved by expansions in spatial eigenfunctions. This form of spectral method gives an efficient solver over a range of Reynolds numbers; cases for $Re \leq 2500$ have been computed. The results are validated by comparing computed pressure and moment coefficients with experimental observations and numerical calculations. In particular, comparisons are made with results from a finite difference method applied to the nonlinear Navier-Stokes equations for which the CPU time is about 400 times that of the present method. The CPU time for the spatial eigenvalue method varies from 10 s at $Re = 10$ to 25 min at $Re = 1000$ on a VAX 8600. The restriction of linear theory is not severe.

I. Introduction

OUR concern is with the internal viscous flow induced when a cylinder filled with fluid spins about an axis performing a coning motion about a second fixed axis. The motivation for our study is to understand the mechanisms that cause a liquid-filled projectile to become aerodynamically unstable when the motion of the projectile induces a resonant response by the fluid. Apart from this application, our investigation is relevant to engineering situations where fluid-filled containers are subject to rotation, e.g., stabilization of satellites by spin. In these situations a resonant response of the fluid will occur when an externally imposed forcing has frequency close to a naturally occurring frequency of oscillation of the fluid. In some cases, the unforced flow has no neutral modes of oscillation, but because the damping rate of a disturbance generally decreases with an increasing Reynolds number, there can still be an unusually large response by the fluid particularly at high Reynolds numbers.

We assume that the motion in the absence of the coning is simply rigid-body rotation. The pivot point of the coning motion will lie at the center of the cylinder. The important cases of "spin-up" and "spin-down" will not be treated. Concepts from hydrodynamic stability are useful in this problem, but discussion of these is left for another paper.

A summary of previous work will be given here; a more detailed summary was given by Sedney.[1] On the basis of inviscid theory, Stewartson[2] calculated the frequencies of free oscillations of a liquid in a spinning cylindrical container and showed that a resonance between these frequencies and the nutational frequency of the projectile causes instability of the projectile. Later, Wedemeyer[3] gave a modified version of Stewartson's theory taking some account of viscous effects. The resulting theory significantly extended the range of applicability of Stewartson's work. The predictions of Stewartson were substantially verified by the observations of Karpov.[4]

Murphy[5] extended Wedemeyer's work by calculating velocity profiles and including the shear-stress term in the moment calculation.

Kitchens et al.[6] applied the ideas of Wedemeyer to satisfy the no-slip condition at the end walls of a rotating cylinder performing small amplitude nutations. Here the forced motion was expressed in terms of a single axial mode of the linear stability problem for solid-body rotation. The nature of Wedemeyer's end-wall correction method means that the work of Kitchens et al. is valid in some approximate sense at high Reynolds numbers. More recently, Gerber et al.[7] investigated the problem again by expanding the disturbed velocity field in terms of trigonometric functions (of complex arguments) in the axial direction. The end-wall conditions were again satisfied approximately by the application of Wedemeyer's technique.

All of the above calculations concern small amplitude motions relevant to a small coning angle of the cylinder. This restriction to the linear regime necessarily means that it is not capable of predicting some flow properties of importance to the projectile stability problem. Although the linear term in the side (or overturning) moment can be calculated, the roll (or despin) moment is zero according to linear theory. (This does not, however, contradict the relations between the side and roll *moment coefficients* as defined by Murphy.[8] See Section IV.) Also, because of the reliance of the above methods on Wedemeryer's method to satisfy the end-wall boundary conditions, the calculations were restricted to large values of the Reynolds number. A primary aim of this paper is to present a method to be used at arbitrarily small Reynolds numbers and to be computationally efficient enough to make extensive parameter studies.

Since this work was begun, alternative numerical approaches have been given. For example, the method of Strikwerda and Nagel[9] is a finite difference method in the axial and radial directions; whereas a spectral method is used in the azimuthal direction. The CPU time is greater by a factor of several hundred for this method compared to that of the present method for $Re < 100$; for $Re \simeq 300$, this finite difference method becomes impractical to run even on a CRAY machine.[10] Comparisons of results from this work and the present work are given.

Herbert[11] uses a spectral-collocation method based on Chebyshev expansions in the axial and radial directions and on a spectral method in the azimuthal direction. The methods of Refs. 9 and 11 are both formulated for an arbitrary coning angle so that nonlinear effects on side and roll moments are evaluated. The method presented here has been extended to

Received Feb. 29, 1988; revision received Nov. 21, 1988.

*Professor of Applied Mathematics.
†Research Scientist. Associate Member AIAA.
††Aerospace Engineer. Member AIAA.

include nonlinear terms, but only results from the linear theory will be presented.

Our solution method is similar to that of Herbert since it can be regarded as a spectral method in which the solution is expanded in the natural eigenfunctions of the problem rather than in Chebyshev polynomials. Our method is based on the eigenfunction expansion approach of Blennerhassett and Hall,[12] which was used to describe the onset of Taylor vortices between concentric cylinders of finite length. The essential idea is to express the disturbance velocity field as a summation over all the linear eigenfunctions of the linear stability problem for solid-body rotation. These eigenfunctions are proportional to $\exp(ikx)$, where k is a wave number and x denotes distance along the cylinders. Thus, k is obtained as an eigenvalue of the ordinary differential system obtained by linearizing the Navier-Stokes equations about solid-body rotation. Actually, an infinite number of eigenvalues of the system exists, and this set of eigenvalues can be, broadly speaking, classified into three subsets. The end wall conditions on the disturbed flow are satisfied by choosing the constants associated with each eigenfunction in the expansion. The convergence of the method can be demonstrated by taking successively more terms in the expansion and noting the behavior of some property. We have no formal proof of convergence of the method, but experience with the Taylor problem suggests that it predicts results consistent with numerical solutions of the Navier-Stokes equations. Indeed, the comparisons made in this paper confirm our belief that the method does converge in a relevant practical range of flow conditions and might, therefore, be of use in other situations such as the spin-up problem.

In Section II we formulate the differential system governing the small amplitude forced motion of a liquid-filled cylinder and express the flow in terms of an eigenfunction expansion. In Section III we explain how the unknown coefficients and eigenvalues in this expansion can be calculated and write down expressions for the pressure and side moment coefficients associated with the motion. In Section IV we give results of several calculations we have performed using the method and compare our predictions with experimental observations and, where possible, results obtained using different approaches. Finally, in an appendix, we explain how the set of eigenvalues of the linear stability problem can be located in the complex wave-number plane using a variety of prediction methods coupled with either a finite difference or with an orthonormalization scheme. This finite difference scheme, to be referenced in Section III, is applied to ordinary differential equations rather than to partial differential equations.

II. Formulation of the Problem

We consider the flow of a viscous fluid of kinematic viscosity υ and density ρ inside a circular cylinder of radius a and half-height $c = Aa$ where A is referred to as the cylinder aspect ratio. We can choose to work in either an inertial frame S or an aeroballistic frame S' with one coordinate axis along the cylinder axis. The main advantage in using S' is that the boundary conditions are easy to apply, but of course, the equations of motion are more complicated. Because we restrict ourselves here to the linear problem where there is no great difficulty in applying the boundary conditions in S, we work in S and choose cylindrical polar coordinate systems (r, θ, x) and (r', θ', x') in S and S', respectively, with the x' axis along the axis of the cylinder, and where x and $x' = 0$ at the midplane. Furthermore, r and x have been made dimensionless using the cylinder radius a.

If K_0 is the angle between the x'-axis and a fixed axis about which the cylinder nutates, then the cylinder has angular velocity $\Omega + \tau\cos K_0$, where Ω is the angular velocity in the aeroballistic frame and τ is the nutational frequency. We define a Reynolds number Re and frequency parameter f by

$$Re = (\Omega + \tau\cos K_0)\, a^2/\upsilon \tag{1a}$$

$$f = \tau/(\Omega + \tau\cos K_0) \tag{1b}$$

The coning angle K_0 is taken to be small throughout the paper; we shall, therefore, be justified in linearizing the Navier-Stokes equations about their solution corresponding to solid-body rotation. Thus, to the order to which we proceed in this paper, we may replace $\cos K_0$ and $\sin K_0$ by 1 and K_0, respectively. There is nothing in our linearized solution to suggest that such a regular expansion in K_0 is nonuniform.

The velocity, pressure, and time variables ($\hat{u}$, $\hat{p}$, and t), appearing in the Navier-Stokes equations, are made dimensionless using the respective scales $(\Omega + \tau)a$, $\rho\, a^2(\Omega + \tau)^2$, and $(\Omega + \tau)^{-1}$. If there is no nutation, the velocity field is given by

$$\hat{u} = (0, r, 0)$$

For small values of K_0, we then construct a solution of the forced problem by expanding the velocity field and pressure as

$$(\hat{u}, \hat{v}, \hat{w}, \hat{p}) = (0, r, 0, r^2/2) + K_0(\hat{u}_0, \hat{v}_0, \hat{w}_0, \hat{p}_0) + 0\,(K_0^2) \tag{2}$$

Because we are using an inertial reference frame, the boundary conditions on the velocity field must be found by a perturbation expansion of the position of the cylinder about its unperturbed ($K_0 = 0$) position. The details of such a calculation are routine and are given in Gerber et al.[7] and lead to

$$\hat{u}_0 = -\text{Real}\,\{i(1-f)x\exp[i(\text{ft} - \theta)]\} \tag{3a}$$

$$\hat{v}_0 = -\text{Real}\,\{(1-f)x\exp[i(\text{ft} - \theta)]\} \tag{3b}$$

$$\hat{w}_0 = +\text{Real}\,\{i(1-f)r\exp[i(\text{ft} - \theta)]\} \tag{3c}$$

at $r = 1$ and at $x = \pm A$.

In addition, it follows from the Navier-Stokes equations, after substituting for $(\hat{u}, \hat{v}, \hat{w}, \hat{p})$ from Eq. (2) and equating terms $0(K_0)$, that (u_0, v_0, w_0, p_0), defined by

$$\hat{u}_0 = \text{Real}\,\{u_0(r, x)\exp[i(\text{ft} - \theta)]\}, \text{ etc.} \tag{4}$$

satisfies

$$i(f-1)u_0 - 2v_0 = -p_{0_r} + (1/Re)[\nabla^2 u_0 - 2u_0/r^2 + 2iv_0/r^2] \tag{5a}$$

$$i(f-1)v_0 + 2u_0 = ip_0/r + (1/Re)[\nabla^2 v_0 - 2v_0/r^2 - 2iu_0/r^2] \tag{5b}$$

$$i(f-1)w_0 = -p_{0_x} + (1/Re)[\nabla^2 w_0 - w_0/r^2] \tag{5c}$$

$$(ru_0)_r - iv_0 + rw_{0_x} = 0 \tag{5d}$$

Here, $\nabla^2 \equiv \partial_x^2 + \partial_r^2 + 1/r\partial_r$, and subscripts r and x denote partial differentiation. The boundary conditions at $r = 1$ and $x = \pm A$ are

$$u_0 = -i(1-f)x, \quad v_0 = -(1-f)x, \quad w_0 = i(1-f)r \tag{6}$$

Thus, the problem for the first-order forced motion is determined by the solution of Eqs. (5) subject to the conditions of Eq. (6) together with the appropriate regularity conditions at $r = 0$. The reduced system, obtained by setting the right side of Eq. (6) equal to zero, has no nontrivial solution; therefore we can seek a solution of the inhomogenous problem by expressing it as a summation over all the eigenfunctions of the unforced problem, which merely satisfy homogenous conditions at $r = 0$, 1. However, it is first convenient to transfer all

the inhomogeneous conditions to the end walls by writing

$$u_0 = -i[1-f]x + u(r,x)$$

$$v_0 = -[1-f]x + v(r,x)$$

$$w_0 = i[1-f]r + \sigma(r) + w(r,x)$$

$$p_0 = -[1-f^2]rx + p(r,x)$$

Here, $\sigma = 2if[r - J_1(\lambda r)/J_1(\lambda)]$ where J_1 is the first order Bessel function of the first kind, and $\lambda = [1+i][(1-f)\,Re/2]^{1/2}$. The boundary conditions on (u, v, w, p) then become

$$u - iv = w = p = 0, \qquad r = 0 \tag{7a}$$

$$u = v = w = 0, \qquad r = 1 \tag{7b}$$

$$u = v = 0,\ w = -\sigma(r), \qquad x = \pm A \tag{7c}$$

The condition of Eq. (7a) ensures that the velocity and pressure remain finite at the center of the cylinder. It remains, therefore, for us to solve Eq. (5) subject to Eq. (6); this is done by expanding (u, v, w, p) above in the form

$$(u, v, w, p) = \sum_{n=1}^{\infty} \frac{\alpha_n \sin k_n x}{\sin K_n A}\,[u_n(r), v_n(r), w_n(r)\cot k_n x,\ p_n(r)] \tag{8}$$

Here $\{\alpha_n\}$ are as yet unknown constants, and it has been assumed in Eq. (8) that u, v, and p are odd functions of x and w is an even function of x. This symmetry is implied by the boundary conditions of Eq. (6) and is consistent with Eq. (3). The eigenvalue k_n and corresponding eigenfunction (u_n, v_n, w_n, p_n) for $n = 1, 2, 3, \ldots$ are determined by the solution of the linearized stability problem for solid-body rotation. This is obtained from Eq. (5) after substituting from Eq. (8) and equating like coefficients of $\sin k_n x$ or $\cos k_n x$. We obtain

$$[Re^{-1}(\Delta_1 - r^{-2}) - iM]u_n + 2[1 + (i/r^2 Re)]v_n - p_{n_r} = 0 \tag{9a}$$

$$[Re^{-1}(\Delta_1 - r^{-2}) - iM]v_n - 2[1 + (i/r^2 Re)]u_n + ip_n/r = 0 \tag{9b}$$

$$[Re^{-1}\Delta_1 - iM]w_n - k_n p_n = 0 \tag{9c}$$

$$(ru_n)_r - iv_n - k_n r w_n = 0 \tag{9d}$$

where $M = f - 1$ and $\Delta_1 \equiv \partial_{rr} + (1/r)\partial_r - [r^{-2} + k_n^2]$.

The boundary conditions are

$$u_n - v_n = w_n = 0 \qquad \text{at } r = 1 \tag{10a}$$

the no-slip condition and

$$u_n - iv_n = w_n = p_n = 0 \qquad \text{at } r = 0 \tag{10b}$$

Equations (9) and (10) constitute an eigenvalue problem for k_n. Since the problem is defined on a finite interval, it is expected that the spectrum will be infinite and discrete. If neutral disturbances were possible, then k would for some n be real; in this problem, the k_n are complex.

We stress at this point that the eigenfunction expansion of Eq. (8), based on the eigenfunctions of the linear stability problem for rigid-body rotation, has not been used previously for the problem under discussion. Elsewhere, it has been used for unstable fluid flows in cylindrical geometries in both the linear and nonlinear regimes; see for example Refs. 12 and 13. The main difficulty with the method is the determination of the set of eigenvalues $\{k_n\}$ and the corresponding eigenfunctions. Without a reasonable guess for the location of these eigenvalues in the complex plane, it would be prohibitively expensive to search for a sufficient number of $\{k_n\}$ each time a flow parameter is varied. We shall describe in the next section how the $\{k_n\}$ and $\{\alpha_n\}$ are found.

III. Determination of the Eigenvalues and the Pressure and Moment Coefficients

The Determination of $\{k_n\}$

Consider the numerical solution of the eigenvalue problem $k_n = k_n(f, Re)$ specified by Eqs. (9) and (10). We assume for the present that a suitable initial guess for k_n is available. We have used two schemes. First, we solved the differential eigenvalue problem by a shooting method coupled to a complete orthonormalization procedure to overcome the stiffness, which develops when Re is large, of Eq. (9). The reader is referred to the paper by Davey[14] for a description of the method; the only essential difference between our equations and those discussed by Davey is that the differential equations here are singular at $r = 0$. We overcame this problem by working out the power series solutions of Eqs. (9) for small r and, hence, determining new conditions on (u_n, v_n, w_n, p_n) at some finite but small value of $r = \epsilon$. A detailed explanation of the implementation of this method to circular flows is given by Kitchens et al.[6] As a check on the above scheme, some calculations were also performed using the scheme of Malik et al.,[15] which is in the class of "finite difference" schemes for solving eigenvalue problems. Results obtained by this method were found to agree well with those obtained by the previous method.

With both methods, a sufficiently accurate guess for k_n was required if the iterations were to converge. This was a hindrance initially because little previous knowledge of the distribution of these eigenvalues was available. To obtain first guesses, techniques were developed to determine approximations to the eigenvalue distribution in certain special limits and, if necessary, to follow their evolution into the required regime.

In the appendix, we describe the different techniques used to locate and classify the spectrum $\{k_n\}$. In fact, it turns out that the spectrum splits into three distinct branches $\{k_{in}\}$, for $i = 1, 2$, and 3. Broadly speaking, the number of zeros of the eigenfunctions associated with k_{in} for $i = 1, 2, 3$ will be roughly equivalent and close to n. Thus, as n increases, the eigenfunctions associated with $\{k_{in}\}$, $i = 1, 2, 3$ develop more oscillations in (0, 1). For the rest of this section, we assume that we have determined the first $N = 3M$ eigenvalue $\{k_n\}$, which has been ordered in the manner outlined above and described in detail in the appendix.

The Determination of $\{\alpha_n\}$

We used two methods to determine the coefficients $\{\alpha_n\}$. First we describe a collocation method and define collocation points $\{r_j\}$ in $[\epsilon, 1]$ with $r_j < r_{j+1}$ and $1 \le j \le M$. Enforcing the boundary conditions of Eq. (7c) at the points $r_1, \ldots, r_M$ leads to

$$E_1(r_j) \equiv \sum_{n=1}^{3M} \alpha_n u_n(r_j) = 0 \tag{11a}$$

$$E_2(r_j) \equiv \sum_{n=1}^{3M} \alpha_n v_n(r_j) = 0 \tag{11b}$$

$$E_3(r_j) \equiv \sum_{n=1}^{3M} (\alpha_n \cot k_n A) w_n(r_j) + \sigma(r_j) = 0 \tag{11c}$$

These $3M$ linear equations are solved for the coefficients $\alpha_1, \ldots, \alpha_{3M}$. The success of the method requires that the α_n and, hence, the flow properties converge in some sense as M increases. Experience has shown that the required value of M to achieve a given accuracy increased monotonically with Re. Numerical examples are given in Section IV.

The second method is a least-squares method. The "normal" equations for α_n are obtained by minimizing the error

$$g(\alpha_n) = \int_0^1 \{|E_1(r)|^2 + |E_2(r)|^2 + |E_3(r)|^2\} r^e \, dr \tag{12}$$

Exponents $e = 0$, 1 gave essentially the same results. A measure of the error, E, in α_n is given by

$$E^2 = g / \int_0^1 |\sigma(r)|^2 r^e dr \tag{13}$$

which is applicable to both methods. Individual measures of error for u, v, and w are defined similarly. They relate to the satisfaction of the end-wall boundary conditions only and, therefore, not to derivatives of u, v, and w that are required in the calculation of the moment. However, they have been useful in evaluating the efficacy of the methods. A discussion of the two methods is given in Section IV where we discuss our results.

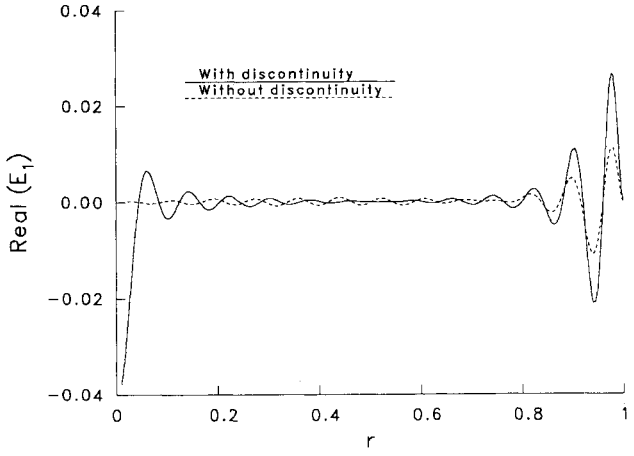

Fig. 1 Real part of the error $E_1(r)$ in the radial velocity u with and without discontinuity at $x = \pm A$, $r = 0$.

Pressure and Moment Coefficients

Having the velocity and pressure from the spatial eigenvalue method, pressure and moment coefficients can be computed and compared with measurements of these quantities. The moment coefficient is used in the study of projectile stability. Only the pressure coefficient on the end wall is considered here. In experiments,[16] pressure transducer measurements are processed to produce amplitude and phase; the amplitude is proportional to the pressure coefficient C_p defined here.

$$C_p = [(p_R + f^2 rx)^2 + p_I^2]^{1/2} \tag{14}$$

where subscripts R and I denote real and imaginary parts of p, respectively; Eq. (14) is derived in Ref. 17. Because the spatial eigenvalue method is semianalytical, useful limiting forms of C_p can be derived as given in Ref. 17. An exact result, even for the nonlinear case, is $C_p = rx$ for $f = 1$.

In general, the motion of the fluid induces three components of moment on the cylinder. The axial component of the moment (despin moment) in the limit of $K_0 \to 0$ is $0(K_0^2)$. Thus, it cannot be predicted by our linear theory, which is valid only up to $0(K_0)$. Notice, however, that the dimensionless definition of this component as given by Murphy[6] contains a factor of K_0^2 in the denominator, which for small K_0 produces a dimensionless roll-moment coefficient of 0(1). In an extension of the work described here to include nonlinear terms, we have continued our calculation up to order K_0^2 to calculate the axial component of the moment.

The transverse components of the moment can be separated into an overturning, or side, moment and an inplane moment, which acts to change the coning rate. We follow Murphy[8] and define a dimensionless side moment C_{LSM} by

$$C_{LSM} = \text{side moment}/[2\pi\rho\, a^4 c(\Omega + \tau)^2 f K_0] \tag{15}$$

Note the factor K_0 in the denominator. Furthermore, Murphy has shown that, after some manipulation, C_{LSM} can be written as

$$C_{LSM} = (fa)^{-1}\left[\int_0^A x p_{0_I}(1,x)\, dx - \int_0^1 p_{0_1}(r, A)\, r^2\, dr\right]$$

$$- (f A\, Re)^{-1} \int_0^A \{[\partial/\partial r\,(x v_{0_R} - w_{0_I})]_{r=1} + 1 - f\} dx$$

$$- (f\, Re)^{-1}\, \text{Real}\{1 - f + \int_0^1 [\partial/\partial x\,(v_0 - i u_0)]_{x=A} r\, dr\} \tag{16}$$

where the subscripts R and I denote real and imaginary parts, respectively. The most likely sources of error in Eq. (16) when using our spectral approach to find (u_0, v_0, w_0, p_0) are the last two terms of Eq. (16) that involve derivatives evaluated at boundaries.

A positive side moment indicates a tendency to increase the coning, or yaw, angle; that is, the projectile is unstable. In almost all cases, the computed C_{LSM} was positive.

IV. Results and Discussion

We briefly describe the steps we took to validate our results. As mentioned previously, we used two schemes for finding the eigenvalue spectrum $\{k_n\}$. The number of zeros in $[\epsilon,1]$ of the eigenfunctions increases with n; therefore the number of grid points needed to calculate the eigenvalues to a prescribed accuracy increases with n. The largest number of eigenvalues used in our calculations was $N = 3M = 108$ for a calculation at a Reynolds number of 2415. The eigenvalues were found to be accurate to at least six decimal places if about 500 grid points were used in $[\epsilon,1]$.

The other crucial part of the calculation is the determination of the constants $\{\alpha_n\}$ using two methods: the collocation and least-squares methods discussed in the previous section. The calculations with either showed that, in order to compute the pressure and moment coefficients to a specified accuracy, the number of eigenvalues used, N, had to be sufficiently large. The flow parameter which essentially governs the required value of N is Re, and, not surprisingly, N increases monotonically with Re. This is to be anticipated since for $Re >> 1$, there will be thin boundary layer regions present in the flow. As an example, we note the whereas $N = 6$ was sufficient to find the pressure and moment coefficients to a given accuracy at $Re = 1$, at $Re = 1000$, $N = 60$ was required. However, calculations with $Re > 1{,}000$ indicated that this rate of increase of N with Re does not continue indefinitely.

In the collocation method, equal spacing (as near as possible) of $\{r_n\}$ was found to be optimum, empirically. Other distributions were used but did not lead to a more rapid rate of convergence of the method. In particular, a scheme, which at the higher values of Re clustered points near $r = 1$ where $\sigma(r)$ has a boundary layer, produced a markedly inferior rate of convergence. We have no explanation for this result, and no rigorous theory appears available to guide our choice of location for the collocation points. No such ambiguity with the least-squares method exists, which uses the computed information at every grid point in $[\epsilon,1]$. We shall refer to programs based on the least-squares and collocation methods as LS and COL in the remainder of this paper.

Finally, we mention a modification which we made to COL to aid its convergence for $Re > 200$. According to the formula-

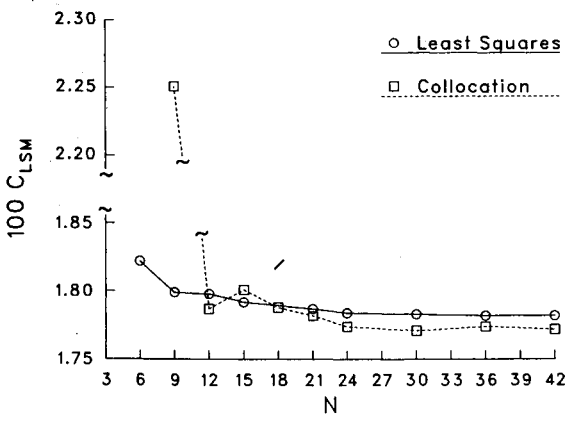

Fig. 2 Moment coefficient vs number of eigenvalues for $Re = 21.5$, $f = 0.0621$, and $A = 1.042$ calculated by LS and COL (note break in ordinate scale).

tion of the problem, u and v are discontinuous at the point $x = \pm A$, $r = 0$. This arises because the no-slip condition on the radial and azimuthal velocity components at $x = \pm A$ is not consistent with (10 b), which requires only that $u_n - iv_n$ vanishes at $r = 0$. In the determination of $\{\alpha_n\}$, we, therefore, applied an extra condition, namely $u + iv = 0$ at $r = \epsilon$ and used an extra eigenvalue k_n in order to achieve this. An illustration of the effect of removing the discontinuity is shown in Fig. 1 using COL. The "error" $E_1(r)$, see Eq. (11), is plotted vs r with the discontinuity present or not. Removing the discontinuity gives a large reduction in E_1 near $r = \epsilon$; a significant reduction is also obtained near $r = 1$. The effect on C_p is relatively small, but on C_{LSM} it is significant.

In Fig. 2 we compare the predictions of LS and COL for C_{LSM} with N in the range $3 \leq N \leq 42$ and $Re = 21.5$, $f = 0.0621$, $A = 1.042$. We find that, as is often the case with spectral methods, the predictions of COL at low values of N are very inaccurate. The least-squares method is accurate at small values of N; for example, the LS value of C_{LSM} at $N = 6$ is within 2% of the converged value. However, we see that the two methods converge to the same value and that the predictions of C_{LSM} are virtually identical for $N \geq 12$. At $N = 42$, the predicted values of C_{LSM} differ by 10^{-4}, which is the limit to the accuracy that can be obtained without further refinement to our eigenvalue calculations.

The type of convergence illustrated above at $Re = 21.5$ is typical of that found for calculations with $Re \leq 200$. At higher Re, the convergence becomes slower so that a large number of eigenvalues have to be calculated. In the range $Re \leq 200$, the converged values predicted by LS and COL always agreed well. For $Re \geq 200$, cancellation of the integrals in Eq. (16) accentuated any numerical errors, but the prediction of C_p did not suffer in the same way. In Fig. 3, we show the dependence of C_p (0.667) on N for $Re = 1000$, $f = 0.1$, and $A = 3$. The predictions of LS and COL differ by less than 1% for $N > 48$. In fact, the converged value predicted by COL and LS is 0.205, and even at $N = 12$, COL predicts a value about 2.5% below this value.

Now we turn to a comparison of our results with available experimental observations and output of other numerical methods. First, we compare our results with some finite difference calculations performed by Nusca[10] using Strikwerda's scheme.

The results we shall give in the remainder of this paper were obtained using sufficient eigenvalues to calculate C_{LSM} and C_p to the graphical accuracy shown. In Fig. 4 we compare C_{LSM} computed by the spatial eigenvalues and finite difference methods for a range of values of Re with $f = 0.1$, $A = 3$, and $K_0 = 2^0$. We noted that the definition of C_{LSM} scales out the dependence of C_{LSM} on K_0 in our linear method; whereas the finite difference calculations allow for the finiteness of K_0.

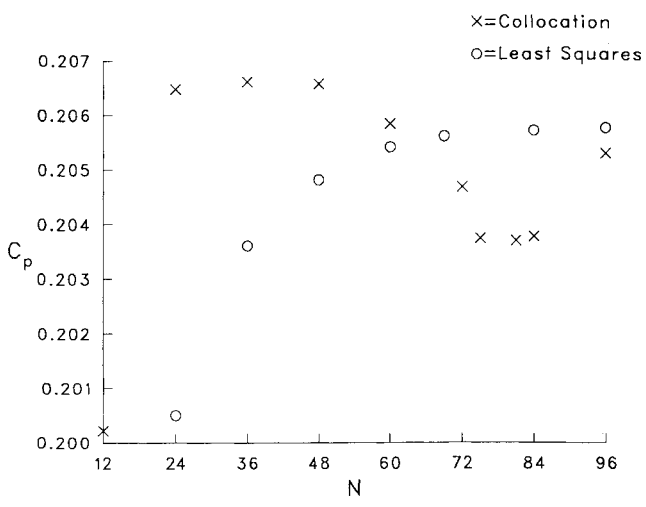

Fig. 3 Pressure coefficient at $r = 0.667$ vs number of eigenvalues for $Re = 1000$, $f = 0.1$, and $A = 3$ calculated by LS and COL.

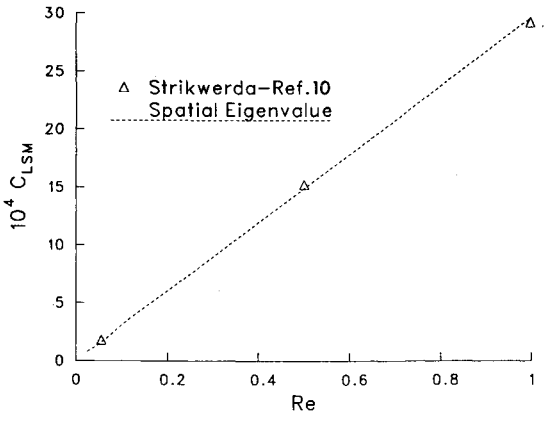

Fig. 4 Moment coefficient vs Re for $f = 0.1$, $A = 3.0$ according to the spatial eigenvalue method and Strikwerda's method, $K_0 = 2$ deg, $0 < Re \leq 1$.

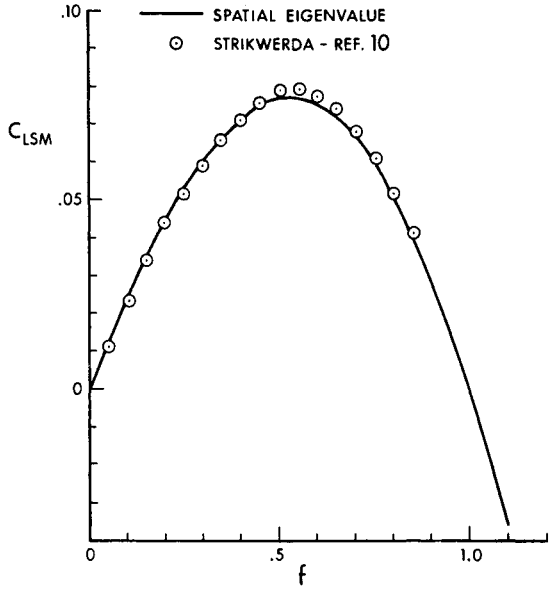

Fig. 5 Moment coefficient vs f for $Re = 10$, $A = 3.0$; $0 \leq f \leq 1.1$ for the spatial eigenvalue results and $0.05 \leq f \leq 0.9$ and $K_0 = 2$ deg for the Strikwerda results.

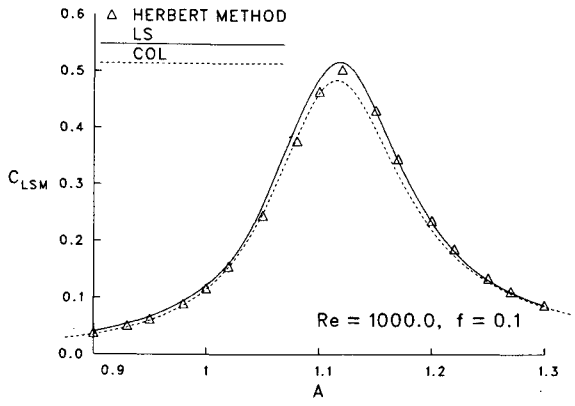

Fig. 6 Moment coefficient vs A for $Re = 1000, f = 0.1, 0.9 \leq A \leq 1.3$ according to the spatial eigenvalue method using LS and COL and including results according to the method of Herbert.

The maximum difference between the calculations occurs at $Re = 1$ and is 0.00003. This difference could be due to lack of numerical resolution in either code or the finiteness of K_0, but in any rate, the difference is too small to be significant here.

Figure 5 shows a similar comparison for the case $A = 3$, $Re = 10$, and $K_0 = 2$ deg with the frequency f varied. The maximum difference is 0.0025 in C_{LSM}, now occurring at $f = 0.6$. The comparisons shown in Figs. 3 and 4 are typical of what we found at Reynolds numbers less than 100 when it was possible to use Strikwerda's code; at higher values of Re, the latter code is prohibitively expensive to be used on a Vax 8600 on which the spatial eigenvalue code was run. No comparison with the earliest finite difference attack on the nonlinear problem by Vaughn et al.[18] was attempted because of the dimensional inhomogeneity in that work pointed out by Nusca.[10]

Apart from lending some support to the validity of our scheme, Fig. 5 also suggests an interesting, previously unsuspected, "resonant"like response of the fluid. This type of response is typical of what is found using the inviscid theory of Stewartson[2]; it is surprising that even at Reynolds numbers as low as 10, this type of response is still possible.

Figure 6 serves a dual purpose: to compare our results with those obtained using T. Herbert's code (data kindly provided by Herbert, private communication) and to present the variation of C_{LSM} vs A for large Re. A more complete discussion of C_{LSM} vs A is given in Ref. 17. The interest in the result lies in the fact that a resonant response is obtained. Although such results are implied in earlier work, none had been presented before. For the parameters of Fig. 6, $Re = 1000, f = 0.1$, the maxima of C_{LSM} at $A = 1.12$, computed by LS and COL, differ by 5%; the maximum obtained by Herbert's method lies between these two values. The difference between our results and those of Herbert are approximately 2%. The cavity, i.e., the liquid-filled cylinder, is tuned by aspect ratio. In previous work on this problem, resonant response tuned by f was investigated. A resonant response is also obtained in the C_p vs A results; the maximum C_p is at $A = 1.12$.

Now that we have in some sense validated our approach, we shall make some comparisons with available experimental results. Again, we note that our approach cannot predict the despin moment so that comparison with, for example, the results of Miller[19] is not possible. In Fig. 7 we compare C_p predicted by the spatial eigenvalue method with some gyroscope data of Hepner et al.[16] The comparison was made at $Re = 3.1$ with $A = 3.148$, $K_0 = 2$ deg, and a range of frequencies. The radius of the cylinder was 3.18 cm, the fluid density was 0.969 gm cm^{-3} with $\upsilon = 60{,}000$ cS. The error estimates in the experimental data were given by Hepner et al. We see that the spatial eigenvalue method slightly underestimates C_p; expect at the highest frequencies shown, the undershoot falls within the experimental error. We have no explanation for this systematic underestimate of C_p; a possible reason is that nonlinear effects might be important in this configuration.

In Fig. 8, C_{LSM} is shown as a function of f for $Re = 2415$, $A = 1.042$, and $K_0 = 2$ deg. Our theoretical results were also compared with the predictions of Gerber and Sedney[20] obtained by using a high Reynolds number approximation. The latter approach produced values approximately 10% below those predicted here. The experimental results are unpublished, kindly supplied to the authors by W.P. D'Amico (pri-

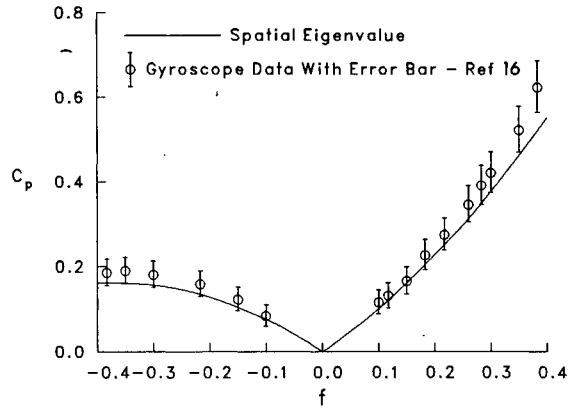

Fig. 7 Calculated pressure coefficient vs f compared with experimental measurements from *Ref.* 16 for $Re = 3.1$, $A = 3.148$, and $r = 0.667$; for the experiment $K_0 = 2$ deg. Estimates of errors in the measurements from Ref. 16 are included.

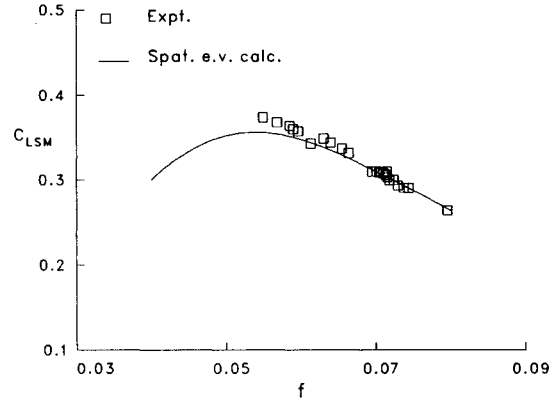

Fig. 8 Moment coefficient vs f for $Re = 2415$, $A = 1.042$ according to the spatial eigenvalue method and measurements of D'Amico (unpublished) with $K_0 = 2$ deg.

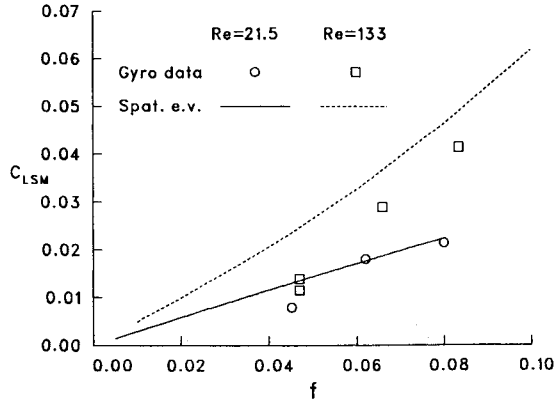

Fig. 9 Moment coefficient vs f for $Re = 21.5$, $A = 1.042$, and $Re = 133.0$, $A = 1.486$ according to spatial eigenvalue method and measurements from Ref. 21 for $K_0 = 2$ deg.

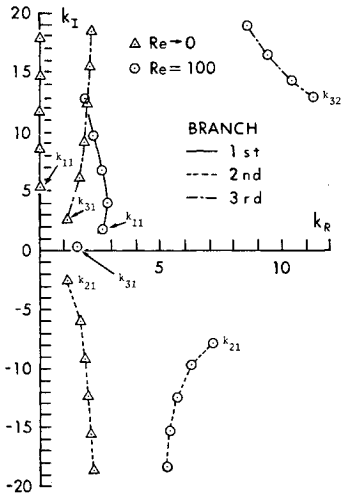

Fig. A1 The first 15 eigenvalues for the Stokes limit and for $Re = 100, f = 0.1$.

vate communication). The computations suggest a resonant response of the fluid not noticed experimentally, presumably, because the frequency was not decreased sufficiently.

Many other comparisons have been made between our computed results and those of Strikwerda's method and with experimental results. The above cases are merely representative; additional cases are given in Ref. 17. Others have not been published but were used for validation of our method. In some instances, errors in both Strikwerda's and experimental results were found by means of these comparisons.

Next a comparison with experimental data is shown in which it is not clear whether the calculation or the experiment gives the correct results. A comparison of calculated side moment coefficients vs f with measurements of D'Amico[21] is shown in Fig. 9 for $Re = 21.5$, $A = 1.042$ and $Re = 133$, $A = 1.486$, both for $K_0 = 2$ deg. The experimental results were deduced from yaw growth rate measurements on a gyroscope. The calculated C_{LSM} is linear for $0 \le f \le 0.035$, approximately. For $Re = 21.5$, the experimental and calculated results agree for the two larger values of f. The reason for the discrepancy at $f = 0.045$ is not known; although, it is pointed out in Ref. 21 that, as C_{LSM} decreases, the error in its measurement increases; no error bounds were presented. For $Re = 133$, the data are uniformly below the calculated results. If extrapolated, the trend of the data implies $C_{LSM} = 0$ for $f = 0.03$, approximately and negative values for $f < 0.03$. In all cases computed thus far, C_{LSM} is positive for $0 < f < 1$. No reason exists for the calculations to become unreliable for these parameters; obtaining error bars for the data is necessary to make a more meaningful comparison. A calculation by Herbert's method would be of value for these parameters.

In conclusion, we note that the method we have developed and tested and that of Herbert are the only numerical schemes available at Reynolds numbers of about 10^3. At lower values of Re, our scheme is much faster than the finitedifference schemes available and could sensibly be used to make extensive parameter studies. Where comparison with other theory has been possible, we have found good agreement; the agreement with experiments was less satisfactory in relatively few cases. Furthermore, the approach is easily extended to take care of nonlinear effects. Some preliminary results in this situation suggest that the disagreement between theory and experiment in Fig. 9 is not due to nonlinear effects.

Another approach, to arrive at an assessment of the linear theory presented here vis-à-vis the nonlinear effects due to "large K_0," is to compare linear spatial eigenvalue results with those from the numerical methods not restricted in K_0. This was attempted in Ref. 17 using finite difference and finite element methods for comparison. The test was frustrated because the results from these two methods disagreed with each other. In spite of this and the small number of cases available for comparison, it appears that the nonlinear effect is small up to $K_0 = 20$ deg.

Appendix

Here we shall briefly describe how initial guesses for the spectrum $\{k_n\}$ can be found.

A Related Taylor Vortex Problem

First, previous knowledge of the eigenvalue distribution for the classical Taylor vortex problem was used.[12] Consider a basic flow driven by the rotation of the cylinder $r = \epsilon$ while the outer cylinder is held fixed. No-slip boundary conditions are applied at $r = \epsilon$ and at $r = 1$. The frequency f and azimuthal wave numbers m are now set to zero. There are three sets of eigenvalues: 1) pure imaginary set $\{k_{3n}\}$, 2) a complex set $\{k_{3n+2}\}$ with $k_{3n+2} = \bar{k}_{3m+1}$ and 3) a complex set k_{3n+1} in the first quadrant with real part $\sim \pi$; $n = 1, 2, \ldots$. Blennerhasset and Hall[12] found that the eigenvalues $\{k_{3n}, k_{3n+1}, k_{3n+2}\}$ have azimuthal velocity eigenfunctions with n zeros in $[\epsilon,1]$. Thus, in the axisymmetric problem, there is a rational method of ordering the eigenvalues, in triplets. If m or f is now taken to be nonzero, the symmetry of the eigenvalue distribution described above is broken, but the ordering from the axisymmetric steady Taylor vortex problem can be retained. The parameters are gradually changed to those of the present problem and the eigenvalues determined numerically. The method was efficient for $Re < 100$. Another approach for small Re, which gives first guesses for an arbitrary number of eigenvalues, is described next.

The Stokes Limit

For values of $Re \le 10$ approximately, estimates for the eigenvalues can be found by solving the $Re \to 0$ problem, i.e., the Stokes limit. Essentially, the same procedure is used as for the classical Stokes flow solution, but $Re \to 0$ is a regular perturbation for the internal flow under consideration. Details are described by Hall et al.[17]

The eigenfunctions $\lim (u_n, v_n, w_n, p_n)$ can be found explicitly in terms of the Bessel functions J_0, J_1, and J_2. The eigenvalues,

$$\lim_{Re \to 0} k_n$$

are the zeros of a transcendental equation involving the same Bessel functions and do not depend on any of the parameters of the problem; these zeros are found using a standard routine. The first several eigenvalues, in this limit, are shown in Fig. A1. They separate into three branches for which the eigenvalues are 1) pure imaginary, 2) in the fourth quadrant, and 3) conjugate to Eq. (2). This is the same separation noted above in the Taylor vortex problem; the bases for this result for that problem and the Stokes limit are completely different, of course.

To indicate this separation, an alternate notation for the eigenvalues $k_{i,n}$ is introduced where $i = 1, 2, 3$ denotes the branch and $n = 1, 2, \ldots$ is the index along a branch. For $n \gg 1$ and using the asymptotic properties of the Bessel functions

$$\lim_{Re \to 0} \text{Im}\,(k_{i,n+1} - k_{i,n}) = \pm \pi$$

with $+$ for $i = 1, 3$ and $-$ for $i = 2$. Empirically, it was found that the eigenvalues for finite Re satisfy the same relation if $n > n_0(Re)$; the function $n_0(Re)$ is only known empirically. Given $k_{i,n}$ for $1 < n < n_0$, using this relation for the imaginary part and extrapolation for the real part provide an effective algorithm for estimating $k_{i,n}$, $n \ge n_0$.

Starting from

$$\lim_{R \to 0} k_{i,n}$$

extrapolating in Re and/or f and using the algorithm, the eigenvalues for any Re and f can be estimated. Relatively large increments in Re can be used for $i = 1$ (in general, it is easier to estimate $k_{1,n}$) but smaller for $i = 2, 3$. Using a systematic extrapolation process, Mermagen[22] constructed a table of $k_{i,n}$ for $0 \le f \le 1$ and $0 \le Re \le 2500$; the estimates were processed through one of the eigenvalue solvers described above so that no further use of the solver is necessary.

Results for $Re = 100$, $f = 0.1$ and $n \le 5$ are shown in Fig. A1. The first eigenvalue on each branch and $k_{3,2}$ are labeled. Note the separation of $k_{3,2}$ and $k_{3,1}$. The ordering of the $k_{i,n}$ is determined by the number of zeros of the eigenfunctions: n zeros corresponding to $k_{1,n}$ and $n - 1$ zeros corresponding to $k_{2,n}$ or $k_{3,n}$.

In calculating the flow variables, the ordering of the $k_{i,n}$ must be preserved; they are taken in groups of three: $i = 1,2,3$ for $n = 1$, $n = 2$, etc. Departure from this ordering introduces errors; the error depends mainly on the degree of departure n and on the method used to calculate α_n.

A more efficient method of estimating $k_{i,n}$, especially $k_{2,n}$ and $k_{3,n}$, for large Re was needed, and for this purpose, asymptotic approximations were derived.

Re→∞

Asymptotic approximations were derived first by assuming $k \sim \kappa_0 + \kappa_1 Re^{-1/2}$ for branch 1 and $k \sim \kappa_0 Re^{1/2} + \kappa_1 Re^{-1/2}$ for branches 2 and 3 with appropriate expansions for the flow variables. Although a boundary layer exists at $r = 1$, it does not enter the calculation of the first two terms for k. The results of the analysis gave suitable first guesses for small n, e.g., $n = 5$ for $Re = 1000, f = 0.1$; see Hall et al.[17] An alternative approach based on the WKB method was derived and gave suitable first guesses, essentially, for all eigenvalues. The solution is in the form of a triple deck with boundary layers of thickness $0(Re^{-1/2})$ at $r = 0$ and $r = 1$ plus the core region for $0 < r < 1$. The eigenfunctions in the boundary layer at $r = 0$ are $Re^{1/4}$ larger than in the core. In the analysis, the mode number n is formally $0(Re^{1/2})$; in practice $n \ge 1$ was used. For example, this method gave first guesses which converged to the eigenvalues $k_{i,n}$ for $Re = 1000$, $f = 0.1$, and $n \ge 1$. However, for $Re = 2415$ and $f = 0.1$, the WKB results converged for $n > 3$; for $n \le 3$, the first mentioned asymptotic method gave the required results. The versatility of the method is shown by the fact that it provides accurate first guesses for $Re \ge 1$ and $n \ge 1$ thereby overlapping the method for $Re \to 0$. Thus, numerical approaches described here provide the means to determine the eigenvalues.

References

[1]Sedney, R., "A Survey of the Fluid Dynamic Aspects of Liquid-Filled Projectiles," AIAA Paper 85-1822-CP, Aug. 1985.

[2]Stewartson, K., "On the Stability of a Spinning Top Containing a Liquid," *Journal of Fluid Mechanics*, Vol. 5, Part 4, Sept. 1959, pp. 577-592.

[3]Wedemeyer, E.H., "Viscous Corrections to Stewartson's Stability Criterion," U.S. Army Ballistic Research Laboratory, Aberdeen Proving Ground, Maryland, BRL Rpt. 1325 (AD489687), June 1966.

[4]Karpov, B.G., "Liquid Filled Gyroscope: The Effect of Reynolds Number on Resonance," U.S. Army Ballistic Research Laboratory, Aberdeen Proving Ground, MD., BRL Rpt. 1302, (AD 479430), Oct. 1965.

[5]Murphy, C.H., "Angular Motion of a Spinning Projectile with a Viscous Liquid Payload," U.S. Army Ballistic Research Laboratory, Aberdeen Proving Ground, MD, ARBRL-MR-03194 (AD A118676) Aug. 1982; also, *Journal of Guidance, Control and Dynamics*, Vol. 6, July-Aug. 1983, pp. 280-286.

[6]Kitchens, C.W., Jr., Gerber, N., and Sedney R., "Oscillations of a Liquid in a Rotating Cylinder: Part I. Solid Body Rotation," U.S. Army Ballistic Research Laboratory, Aberdeen Proving Ground, MD, ARBRL-TR-02081 (AD A057759), June 1978.

[7]Gerber, N., Sedney, R., and Bartos, J.M., "Pressure Moment on a Liquid-Filled Projectile: Solid Body Rotation," U.S. Army Ballistic Research Laboratory, Aberdeen Proving Ground, MD, ARBRL-TR-02422 (AD A120567), Oct. 1982.

[8]Murphy, C.H., "A Relationship Between Liquid Roll Moment and Liquid Side Moment," U.S. Army Ballistic Research Laboratory, Aberdeen Proving Ground, MD, ARBRL-MR-03347 (AD A140658), April 1984.

[9]Strikwerda, J.C., and Nagel, Y.M., "A Numerical Method for Computing the Flow in Rotating and Coning Fluid-Filled Cylinders," Aberdeen Proving Ground, MD, CRDC-SP-85006 (AD B094742), Nov. 1984.

[10]Nusca, M.J., "Computational Fluid Dynamics Methods for Low Reynolds Number Precessing/Spinning Incompressible Flows," U.S. Army Ballistic Research Laboratory, Aberdeen Proving Ground, MD, BRL-MR-3657 (AD A193891), April 1988. Also, Nusca, M.J., private communication.

[11]Herbert, T., and Li, R., "Numerical Study of the Flow in Spinning and Nutating Cylinder," AIAA Paper 87-1445, June 1987.

[12]Blennerhasset, P.J., and Hall, P., "Centrifugal Instabilities of Circumferential Flow in Finite Cylinders: Linear Theory," *Proceedings of the Royal Society of London*, Series A, Vol. 365, 1979, pp. 191-207.

[13]Hall, P., "Centrifugal Instabilities of Circumferential Flows in Finite Cylinders: Nonlinear Theories," Proceedings of the Royal Society of London, Series A, Vol. 372, 1980, pp. 317-356.

[14]Davey, A., "A Simple Numerical Method for Solving Orr-Sommerfeld Problems," *Quarterly Journal of Mathematics and Applied Mechanics*, Vol. 26, Part 4, 1973, pp. 401-411.

[15]Malik, M.R., Chuang, S., and Hussaini, M.Y., "Accurate Numerical Solution of Compressible, Linear Stability Equations," *Journal of Applied Mathematics and Physics (ZAMP)*, Vol. 33, March 1982, pp. 189-201.

[16]Hepner, D.J., Kendall, T.M., Davis, B.S., and Tenly, W.Y., "Pressure Measurements in a Liquid-Filled Cylinder Using a Three-Degree-of-Freedom Flight Simulator," U.S. Army Ballistic Research Laboratory, Aberdeen Proving Ground, MD, BRL-MR-3560, Dec. 1986.

[17]Hall, P., Sedney, R., and Gerber, N., "Fluid Motion in a Spinning, Coning Cylinder via Spatial Eigenfunction Expansion," U.S. Army Ballistic Research Laboratory, Aberdeen Proving Ground, MD, ARBRL-TR-2813 (AD A190758), Aug. 1987.

[18]Vaughn, H.R., Oberkampf, W., and Wolfe, W.R., "Fluid Motion Inside a Spinning Nutating Cylinder," *Journal of Fluid Mechanics*, Vol. 150, 1985, pp. 121-138. Also "Numerical Solution for a Spinning, Nutating Fluid-Filled Cylinder," Sandia Rpt. SAND 83-1789, Dec. 1983.

[19]Miller, M.C., "Measurements of Despin and Yawing Moments Produced by a Viscous Liquid," *Journal of Guidance, Control, and Dynamics*, Vol. 8, No. 2, March-April 1985, pp. 282-284.

[20]Gerber, N., and Sedney, R., "Moment on a Liquid-Filled Spinning and Nutating Projectile: Solid Body Rotation," U.S. Army Ballistic Research Laboratory, Aberdeen Proving Ground, MD, ARBRL-TR-02470 (AD A125332), Feb. 1983.

[21]D'Amico, W.P., "Instabilities of a Gyroscope Produced by Rapidly Rotating, Highly Viscous Liquids," AIAA Paper 81-0224, Jan. 1981; also, *Journal of Guidance, Control and Dynamics*, Vol. 7, No. 4, July-August 1984, pp. 443-449.

[22]Mermagen, W.H., private communication, U.S. Army Ballistic Research Laboratory, Aberdeen Proving Ground, MD.